Impacts of K-12 school reopening on the COVID-19 epidemic in Indiana, USA

Guido España[#], Sean Cavany[*], Rachel Oidtman[*], Carly Barbera,
Alan Costello, Anita Lerch, Marya Poterek, Quan Tran, Annaliese Wieler
Sean Moore, T. Alex Perkins[#]

Department of Biological Sciences and Eck Institute for Global Health,
University of Notre Dame, United States
[#]Correspondence: guido.espana@nd.edu, taperkins@nd.edu
[*]Equal contribution

Key points

Question: What will be the impact of reopening schools on SARS-CoV-2 infections and COVID-19 mortality in Indiana?
Findings: Reopening schools at full capacity with low (50%) face-mask adherence could have a substantial effect on the burden of COVID-19 across Indiana, leading to 83 times more infections and 13 times more deaths than if schools operated remotely. Reopening at 50% capacity and with increased face-mask adherence (100%) could mitigate much of this risk, leading to 12% more infections and 5% more deaths than if schools operated remotely.
Meaning: Schools should make efforts to reduce capacity and enforce face-mask adherence to prevent increases in the statewide burden of COVID-19.

Abstract

Importance: In the United States, schools closed in March 2020 to reduce the burden of COVID-19. They are now reopening amid high incidence in many places, necessitating analyses of the associated risks and benefits.
Objective: To determine the impact of school reopening with varying levels of operating capacity and face-mask adherence on COVID-19 burden.
Design: Modeling study using an agent-based model that simulates daily activities of the population. Transmission can occur in places such as schools, workplaces, community, and households. Model parameters were calibrated to and validated against multiple types of COVID-19 data.
Setting: Indiana, United States of America.
Participants: Synthetic population of Indiana. K-12 students, teachers, their families, and others in the state were studied separately.

Interventions: Reopening of schools under three levels of school operating capacity (50%, 75%, and 100%), as well as three assumptions about face-mask adherence in schools (50%, 75%, and 100%). We compared the impact of these scenarios to reopening at full capacity without face masks and a scenario with schools operating remotely, for a total of 11 scenarios.
Main outcomes: SARS-CoV-2 infections, symptomatic cases, and deaths due to COVID-19 from August 24 to December 31.
Results: We projected 19,527 (95% CrI: 4,641-56,502) infections and 360 (95% CrI: 67-967) deaths in the scenario where schools operated remotely from August 24 to December 31. Reopening at full capacity with low face-mask adherence in schools resulted in a proportional increase of 81.7 (95% CrI: 78.2-85.3) times the number of infections and 13.4 (95% CrI: 12.8-14.0) times the number of deaths. High face-mask adherence resulted in a proportional increase of 3.0 (95% CrI: 2.8-3.1) times the number of infections. Reducing capacity with high face-mask adherence resulted in only a 11.6% (95% CrI: 5.50%-17.9%) increase in the number of infections.
Conclusions and Relevance: Reduced capacity and high face-mask adherence in schools would substantially reduce the burden of COVID-19 in schools and across the state. We did not explore the impact of other reopening scenarios, such as alternating days of attendance. Heterogeneous decisions could be made across different districts throughout the state, which our model does not capture. Hence, caution should be taken in interpreting our results as specific quantitative targets for operating capacity or face-mask adherence. Rather, our results suggest that schools should give serious consideration to reducing capacity as much as is feasible and enforcing adherence to wearing face masks.

1 Introduction

The United States has been the country most severely impacted by the COVID-19 pandemic in terms of total reported cases and deaths, with over 5.2 million cases and 167,000 deaths by August 14 [1]. This severity led to social interventions on an unprecedented scale, including restrictions on mass gatherings, bans on non-essential travel, and school closures [2, 3, 4, 5]. While such restrictions were initially successful in reducing transmission, the subsequent relaxation of restrictions on mass gatherings and movement were followed by large increase in notified cases and, more recently, deaths [1, 3, 6, 7]. The state of Indiana reported its highest daily number of cases to date (1,249) on August 6 [8].

It is within this context of intense community transmission that attention has turned to the reopening of schools for the start of the academic year in August [9, 10, 11]. During influenza epidemics, school closures have been estimated to reduce transmission community-wide [12, 13, 14]. In general, schools are seen as key drivers of the transmission of respiratory pathogens due to close contact among children at school [15, 16, 17]. However, several factors complicate the effect of school reopenings on SARS-CoV-2 transmission. In particular, children and adolescents appear less susceptible to infection and are much less likely to experience severe outcomes following infection [18, 19, 20, 21, 22, 23]. It is also still unclear what their contribution to transmission is, but several studies suggest they can play an important role [18, 24, 25, 26]. There are additional economic and social factors to consider, too, such as the economic costs of school closures for

families that must then stay home from work, and the nutritional benefits of school reopening for children who rely on free and subsidized school meals [27, 28, 29].

Our objective in this study was to explore the impacts of strategies for school reopening on the burden of COVID-19 in the state of Indiana, USA. We synthesized evidence around features of COVID-19 epidemiology in children [19] in an agent-based model originally developed for pandemic influenza [30] that is equipped to translate such evidence into projections of community-wide transmission under alternative scenarios about school reopening. We focused on the role of reducing the capacity of classrooms and adherence with wearing face masks in schools, given that both physical distancing and face masks have been shown to reduce transmission of SARS-CoV-2 in community settings [31]. Our main outcome measures were changes in statewide totals of SARS-CoV-2 infections, symptomatic infections, and deaths, across different scenarios of school capacity and face-mask adherence, compared with keeping schools closed.

2 Methods

Approach

Our approach to modeling SARS-CoV-2 transmission is based on the Framework for Reconstructing Epidemic Dynamics (FRED) model [30]. Using this model, we simulated the spread of SARS-CoV-2 in the population of Indiana, USA using a synthetic population with demographic and geographic characteristics of the population, including age, household composition, household location, and occupation [32]. We analyzed the impact of school reopening from August 24 to December 31, 2020 in the overall population of Indiana, as well as in students, teachers, and their households. We quantified impact as the difference in the number of COVID-19 infections, symptomatic infections, and deaths, between each scenario and the baseline scenario.

Agent-based model

We chose an agent-based model for this analysis to address key issues such as heterogeneity of transmission within a population due to population density, age, occupation, and contact network. We used synthetic populations of Indiana to realistically represent characteristics of the population [32]. FRED simulates pathogen spread in a population by recreating interactions among people on a daily basis. Each human is modeled as an agent who visits a set of places defined by their activity space (houses, schools, workplaces, and neighborhood locations). Transmission can occur when an infected person visits the same location as a susceptible person on the same day, with numbers of contacts per person specific to each location type. For instance, school contacts depend not on the size of the school but on the age of the student. Every day of the week, students and teachers visit their school, and students are assigned to classrooms based on their age. Given that schools are closed during the weekends, community contact is increased by 50% [30]. For both schools and other locations, we adopted contact rates for each location type that were previously calibrated to attack rates for influenza specific to each location type [30, 33].

Once infected, each individual had latent and infectious periods drawn from distributions calibrated so that the average generation interval distribution matched estimates from Singapore (mean = 5.20, standard deviation = 1.72) [34]. The absolute risk of transmission depended on the number and location of an infected individual's contacts and a parameter that controls SARS-CoV-2 transmissibility upon contact, which we calibrated. A proportion of the infections were asymptomatic [35]. We assumed these infections were as infectious as symptomatic infections and had identical incubation and infectious period distributions [36, 37, 26, 38]. We assumed that children were less susceptible to infection than adults, which we modeled with a logistic function calibrated to model-based estimates of this relationship by Davies et al. [19]. We assumed that severity of disease increased with age, consistent with statistical analyses performed elsewhere [39, 40, 41, 21].

Agent behavior in FRED has the potential to change over the course of an epidemic. Following the onset of symptoms, infected agents self-isolate at home according to a fixed daily rate, whereas others continue their daily activities [42, 43]. This rate was chosen so that, on average, 68% of agents will self-isolate at some point during their symptoms, assuming that all individuals who develop a fever will isolate at some point during their symptoms. Agents can also respond to public health interventions, including school closure, shelter in place, and a combination of mask-wearing and social distancing. School closures occur on specific dates [44], resulting in students limiting their activity space to household and neighborhood locations. Shelter-in-place interventions reduce some agents' activity spaces to their households only, whereas others continue with their daily routines. We used mobility reports from Google [45] to drive daily compliance with shelter-in-place, such that shelter-in-place compliance in our model accounts for both the effects of shelter-in-place orders and some people deciding to continue staying at home after those orders are lifted [46]. To account for voluntary mask-wearing and social distancing, we used Google Trends data for Indiana using the terms "face mask" and "social distancing" [47]. Face mask compliance was informed by estimates of face-mask adherence from survey data [48]. Further details about the model are available in the Supplementary Text.

Data and outcomes

We obtained daily incidence of death from the New York Times COVID-19 database [1]. Hospitalizations and the age distribution of deaths reported in Indiana were obtained from the Indiana COVID-19 dashboard [8]. Daily numbers of tests performed in the state were available from The Covid Project [49]. We calibrated the model to daily values of deaths, hospitalizations, and test positivity through August 10 and to the age distribution of deaths cumulative through July 13 to estimate nine model parameters using a sobol design sampling algorithm [50, 51] (Supplementary Material). We validated the model by comparing its predictions of the infection attack rate (IAR) and IAR by age to results from two statewide serological surveys undertaken in late April and early June [52, 53].

To account for uncertainty in the calibrated parameters in our future projections, we simulated nine scenarios about school reopening with values of the model's nine free parameters sampled from the calibrated distribution. From August 24 to December 31, we outputted numbers of daily infections, symptomatic cases, hospitalizations, and deaths, structured by age, place

of infection (school, home, other), and affiliation with schools (student, teacher, none). For our analysis, we focused on the infections, symptomatic cases, and deaths in the overall population and the subgroups of students, teachers, and their families.

We explored three scenarios for school capacity (50%, 75%, or 100% of students receiving in-person instruction) and three scenarios for face-mask adherence in schools (50%, 75%, or 100%). We compared each of the nine combinations of these scenarios to a scenario in which schools reopened normally (100% capacity, 0% face-mask adherence) and to a scenario in which schools remained closed until the end of the year. We analyzed the sensitivity of the model outcomes to parameter uncertainty by calculating the partial rank correlation coefficient of each calibrated parameter and two outcomes: the cumulative number of infections between August 24 and December 31, and the proportion of infections acquired in schools during that period.

3 Results

Our model was generally consistent with the data to which it was calibrated, capturing trends over time in daily deaths, hospitalizations, and test positivity (Fig. 1A-C), as well as greater proportions of deaths among older age groups (Fig. 1D). Some trade-offs in the model's ability to recreate different data types were apparent, such as a recent increase in hospitalizations that the model failed to capture (Fig. 1C), likely due to the predominance of data on deaths in the likelihood. Even so, the model's predictions reproduced the range of variability in the data, as assessed by coverage probability of its 95% posterior predictive intervals (daily deaths: 0.91; daily hospitalizations: 1.0; daily test positivity: 0.97; cumulative deaths by age: 1.0). The model was also consistent with data withheld from fitting. Across all ages, the 95% credible intervals of infection attack rates (IAR) through late April (median: 0.0174; 95% CrI: 0.0058-0.064) and early June (median: 0.0221; 95% CrI: 0.0072-0.08) from two state-wide serological surveys [52] fell within the 95% posterior predictive intervals of our model (Fig. S1A). Our model's predictions also overlapped with age-stratified estimates of IAR from those serological surveys (Fig. S1B), although it underpredicted IAR among individuals aged 40-60 years.

Calibration of the parameter that scaled the magnitude of SARS-CoV-2 importations [54, 55] in our model resulted in a median of 1.118 (95% PPI: 0.654-1.456) imported infections per day from February 1 to August 10. To ensure that the model reliably reproduced the high occurrence of deaths observed in long-term care facilities, we seeded infections into those facilities at a daily rate proportional to the prevalence of infection on that day; this calibrated proportion was 0.046 (95% PPI: 0.007-0.093). On the opposite end of the age spectrum, our calibration resulted in a median estimate of susceptibility among children of 0.357 (95% CrI: 0.263-0.526), compared to 0.788 (95% CrI: 0.651-0.946) in adults (Fig. S2). Our calibration resulted in an estimate of transmissibility (median: 0.641; 95% CrI: 0.546-0.965) that corresponded to values of $R(t)$ during the initial phase of the epidemic in Indiana of 1.67 (95% CrI: 0.47-3.57), which represents an average of daily values across the month of February (Fig. 1A). Driven by a calibrated estimate that the proportion of people sheltering in place rose in early March and peaked at a median of 38.2% (95% CrI: 25.2-68.7%) on April 7 (Fig. S3A), our estimates of $R(t)$ dropped to a low of 0.57 (95% CrI: 0.41-0.75) on April 7 and have remained below 1 since (Fig. 1A). Also impacting

our estimates of $R(t)$ is the increasing use of face masks in the community, which we estimated

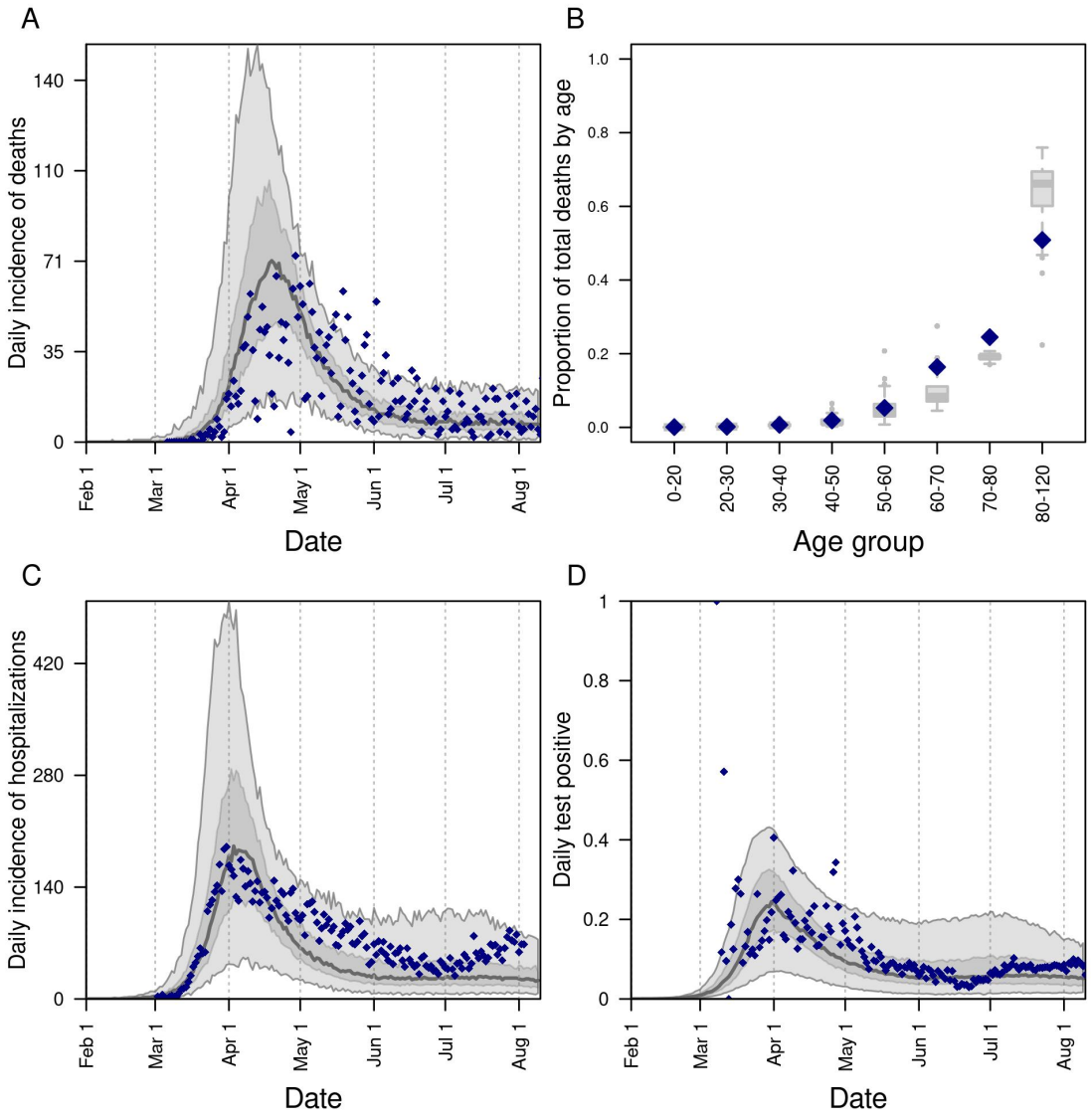

Figure 1. Model calibration to data: A) daily incidence of death; B) proportion of deaths through July 13 in decadal age bins; C) daily incidence of hospitalization; and D) daily proportion of tests administered that are positive for SARS-CoV-2. In all panels, blue diamonds represent data. In A, C, and D, the gray line is the median, the dark shaded region the 50% posterior predictive interval, and the light shaded region the 95% posterior predictive interval.

at 0.50 (95% CrI: 0.458-0.545) as of July 19 (Fig. S3B). Note that this estimated distribution of community face-mask adherence does not differ between scenarios and is not the same as the level of adherence in schools, which we imposed at different levels depending on the scenario.

In the event that schools reopen at full capacity and without any use of face masks, our model projects that $R(t)$ would increase to 1.94 (95% CrI: 1.47-2.20) by mid-September (Fig. 2A). This assumes that levels of sheltering in place and face-mask adherence in the community remain at their estimated levels as of August 13 (Fig. S3B). Consistent with our model's prediction that schools contributed appreciably to transmission early in the epidemic (median: 24.6%; 95% CrI: 23.2-27.7%), this increase in transmission is associated with an increase in the proportion of infections arising in schools upon their reopening (Fig. 2B). The sensitivity of the proportion of infections arising in schools to model parameters was highest for the inflection point of the age-susceptibility relationship, the transmissibility parameter, and the rate at which infections were imported into long-term care facilities (Fig. S7). This increase in infections arising in schools is projected to give rise to additional transmission statewide (Fig. 2C). An example of transmission chains arising from schools and spilling out into school-affiliated families and the broader community is shown in Fig. 3.

In the event that schools remain open throughout the semester and no other policies or behavioral responses occur, the increase in $R(t)$ driven by reopening schools at full capacity and without the use of face masks would be projected to result in 2.49 million (95% CrI: 2.08-2.70 million) infections (Fig. 4A) and 9,117 (95% CrI: 6,117-6,248) deaths (Fig. 4B) from Indiana's population as a whole between August 24 and December 31. At the other extreme, if schools were to go to remote instruction and all children remained at home, our model projects that $R(t)$ would remain near current levels through the remainder of 2020 (Fig. S4A). Again, this assumes that levels of sheltering in place and face-mask adherence in the community as a whole remain at their estimated levels as of August 13. Under this scenario, transmission would continue through contacts at workplaces, within homes, and elsewhere in the community (Fig. S4B), with 19,527 (95% CrI: 4,651-56,502) infections (Fig. S4C) and 360 (95% CrI: 67-967) deaths between August 24 and December 31.

Differing policies on the capacity at which schools operate in person and enforce the use of face masks have a strong influence on the projected statewide burden of COVID-19. If schools operate at 50% capacity and achieve high face-mask adherence, the number of infections and deaths that we project is similar to what we project under the scenario in which schools operate remotely (Fig. 4, Table S1). Of these two policies, projections of infections and deaths were more sensitive to the capacity at which schools operate, with the worst outcomes projected to occur when schools operate at full capacity and with low face-mask adherence. Under this scenario, cumulative infections statewide were projected to be 300% (95% CrI: 280-310%) greater than if schools operated remotely, and cumulative deaths statewide were projected to be 50% (95% CrI: 50-60%) greater (Table S1). The sensitivity of these results to model parameters was relatively high for parameters that define the age-susceptibility relationship and, in some cases, for the transmissibility and shelter-in-place compliance parameters (Fig. S6).

The burden of COVID-19 associated with reopening schools differed for students, teachers, and their families. Relative to a scenario with remote instruction, risk of infection and symp-

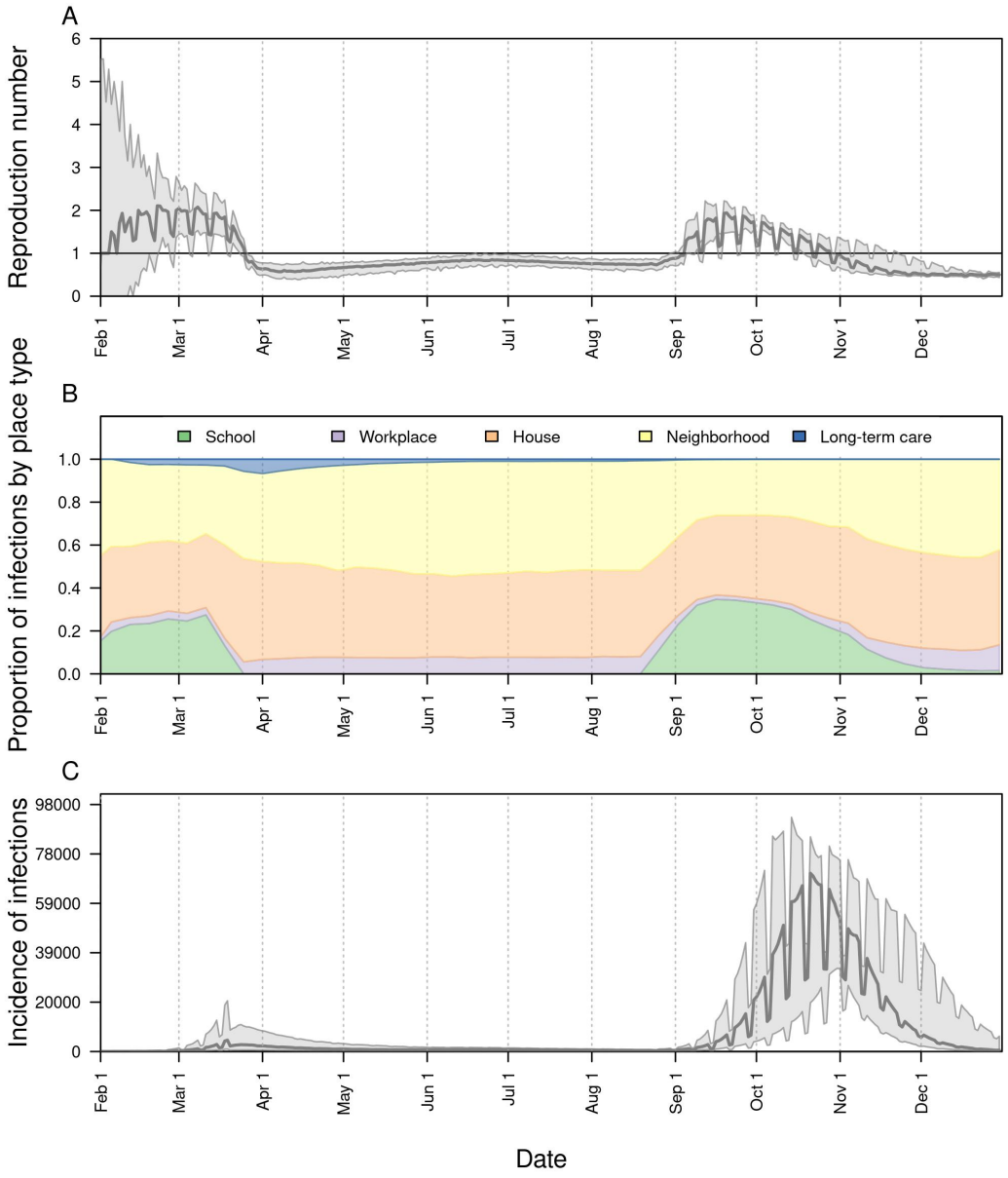

Figure 2. The impact of school reopening in Indiana on: A) the reproduction number, $R(t)$, over time; B) the proportion of infections acquired in different location types over time; and C) the daily incidence of infection over time. In all panels, schools reopened on August 24. In A and C, the line represents the median, and the shaded region represents the 50% posterior predictive interval.

tomatic infection was greatest for students (Fig. 5, left column), with a hundred-fold or greater increase in the risk of infection if schools operate at full capacity with moderate or low face-mask adherence (Table S2). Due to their older ages, teachers and families experienced a much higher risk of death under scenarios with high capacity and moderate or low face-mask adherence, as compared with a scenario with remote instruction (Fig. 5, center & right columns). Under a scenario with high capacity and low face-mask adherence, there was a 227-fold higher risk of death for teachers (Table S3) and a 266-fold higher risk of death for family members (Table S4). At the same time, the risk of death under a scenario with high capacity and low face-mask adherence was around half the risk of death if schools were to operate at full capacity with no masks (Tables S7 & S8).

4 Discussion

Our model provides a detailed, demographically realistic representation of SARS-CoV-2 transmission in Indiana that is consistent both with data to which it was calibrated and to data that was withheld from calibration. In contrast to models that rely on assumptions about intervention impacts or estimate them statistically [2, 56], our model makes predictions about intervention impacts based on first-principles assumptions about individual-level behavior and contact patterns. Consistent with results from other analyses [2, 56, 20], the inputs and assumptions in

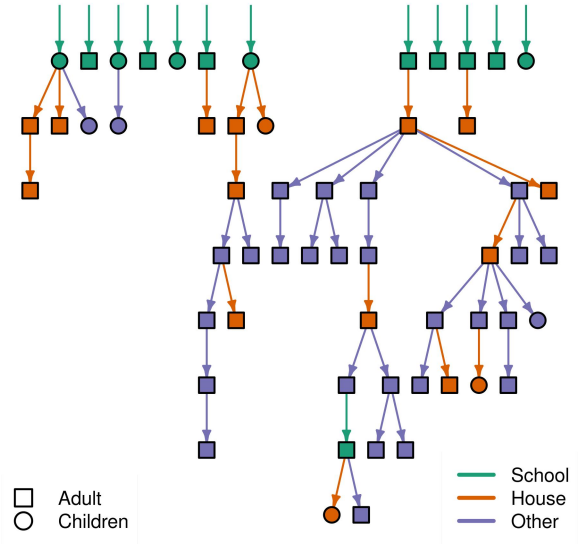

Figure 3. Example transmission tree of SARS-CoV-2 from one simulation of the model for Saint Joseph County, Indiana. Green shapes at the top represent agents in the model infected at school, and arrows descending from them and other shapes show transmission events in school-affiliated households (orange) and the community at large (purple) that trace back to infections originally acquired in schools. Different shapes distinguish children (circles) from adults (squares).

our model led to a prediction that schools made a considerable contributions to SARS-CoV-2 transmission in February and early March, prior to large-scale changes in behavior. Extending that, a primary result of our analysis is that schools could, once again, make a considerable contribution to SARS-CoV-2 transmission if they resume normal activity in the fall semester.

Our results indicate that operating at reduced capacity and achieving high face-mask adherence would reduce the burden of COVID-19 in schools and across the state. In the event that both interventions are pursued fully, our model projects that infections and deaths statewide would be around 10% greater than under a scenario with fully remote instruction. In the event that schools operate at full capacity, our model projects that infections and deaths statewide could be one to two orders of magnitude greater than under a scenario with fully remote instruction, especially if there is poor face-mask adherence in schools. The impacts associated with reducing capacity result from reductions in both the number of contacts within the school and the probability that an infected student would be in attendance in the first place, similar to the logic behind why smaller gatherings are associated with reduced risk of transmission [3, 57, 58].

Although the scenarios we considered resulted in projected impacts spanning nearly the full range between fully remote instruction and fully in-person instruction with no face masks, they are a simplification of the full range of scenarios of how schools could operate this fall. Scenarios

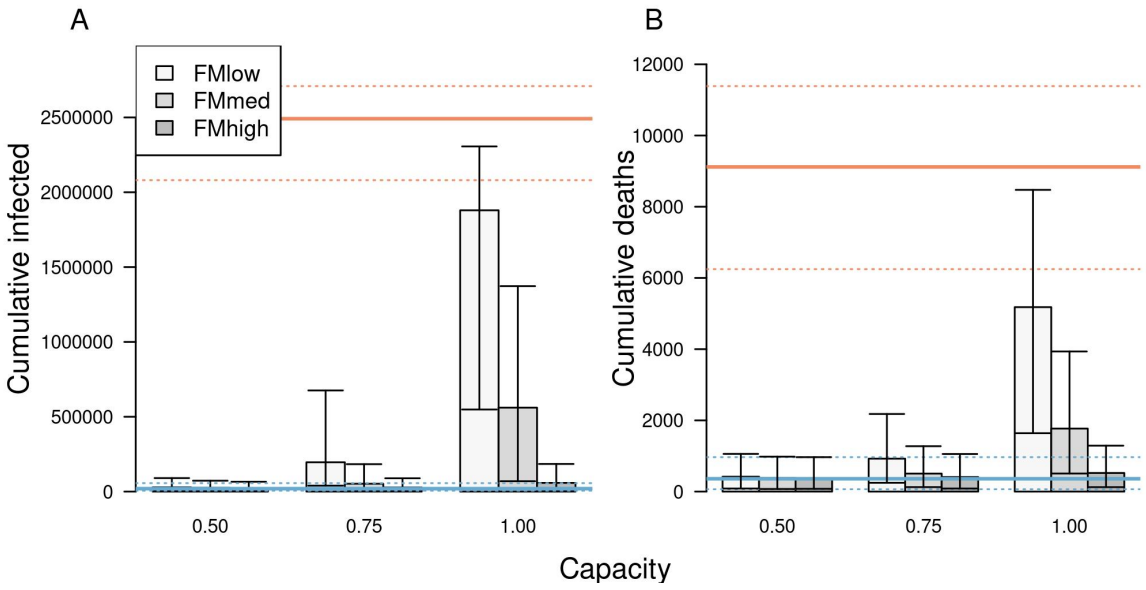

Figure 4. The impact of different school reopening strategies on A) cumulative infections and B) cumulative deaths in Indiana between August 24 and December 31. Scenarios are defined by the capacity at which schools operate (x-axis) and face-mask adherence (shading). Orange lines represent projections under a scenario of school reopening at full capacity without masks (solid: median; dotted: 95% posterior predictive interval). Blue lines represent a scenario where schools operate remotely. Error bars indicate inter-quartile ranges.

that we did not explore include different groups of students attending in-person or remotely [59], varying degrees of modularization within schools [60], and the implementation of testing-based control strategies in schools [61]. A related simplification of our statewide analysis is that the state will, in reality, consist of a patchwork of policies across districts. In light of this complexity that our model does not capture, our results should be interpreted with caution in setting specific, quantitative targets for capacity or face-mask adherence. For any scenario though, our results illustrate the importance of reducing capacity and maximizing face-mask adherence to the extent possible, as do other modeling studies [59, 60, 61, 62, 63].

The burden of COVID-19 associated with reopening schools is not expected to fall evenly across the state's population. Under scenarios with schools operating at full capacity, our model projects that hundreds of thousands of children could be infected during the fall semester. Whereas very few deaths are expected among infected children, the numbers of deaths among teachers and school-affiliated families could number in the hundreds. In comparison, the total number of deaths projected across the state is projected to be in the low thousands, meaning that adults with close ties to schools could represent a sizable fraction of deaths across the state in coming months, if schools operate at full capacity and with low face-mask adherence. Importantly, the magnitude of these projections depend further on factors outside the control of schools [2]. In the absence of school reopening, our projections assume steady, controlled levels of transmission with $R(t) < 1$. Changes in government policies, individual behavior, and face-mask adherence in the community all have the potential to alter this trajectory for the state as a whole, as well as its schools [2, 31, 64].

A critical assumption of our analysis is that children are capable of being infected with SARS-CoV-2 and transmitting it to others at meaningful levels. Although the burden of severe disease skews strongly towards older ages [22, 65, 8], there are other lines of evidence that support our assumption. These include a contact-tracing study that found no distinguishable difference between infectivity of children and adults [26], several studies that found no distinguishable difference in viral load between children and adults [66, 37, 36, 67], a study that observed a greater secondary attack rate among children in homes [26], and a modeling study that found no evidence that children were less infectious [68]. More direct evidence comes from COVID-19 outbreaks that have already been observed in schools, including one in a high school in Israel in which 13.2% of students and 16.6% of staff were infected in just 10 days [69]. Even more pertinent, some schools in Indiana recently reopened and have already reported cases of COVID-19 among students [70]. Our analysis offers perspective on what those initial cases could give rise to in coming months, depending on the degree to which schools choose to operate at reduced capacity and enforce face-mask adherence.

There is now a growing body of evidence that school closures contributed to mitigating the first wave of the epidemic and could lead to rising case numbers if relaxed [6, 61]. Our study adds to this evidence, and suggests an even greater impact of school reopening than several other studies [63, 61, 60, 71, 59]. This is due in part to our assumption that asymptomatic and symptomatic infections contribute similarly to transmission [26, 66, 37, 36, 67], and in part to our model's ability to capture chains of transmission within schools and extending out into the community. Our study echoes several modeling studies in emphasizing the importance of

reducing school capacity to impede transmission [60, 61, 62, 63, 71]. Taking all this evidence together, those deciding on strategies to safely reopen schools should strongly consider operating at reduced capacity and strictly enforcing face-mask usage. Both schools, and the communities in which they are embedded, stand to be affected by these policy choices.

5 Acknowledgements

This work was supported by an NSF RAPID grant to TAP (DEB 2027718), an Arthur J. Schmitt Fellowship and Eck Institute for Global Health Fellowship to RJO, and a Richard and Peggy Notabaert Premier Fellowship to MP. We thank the University of Notre Dame Center for Research Computing for computing resources.

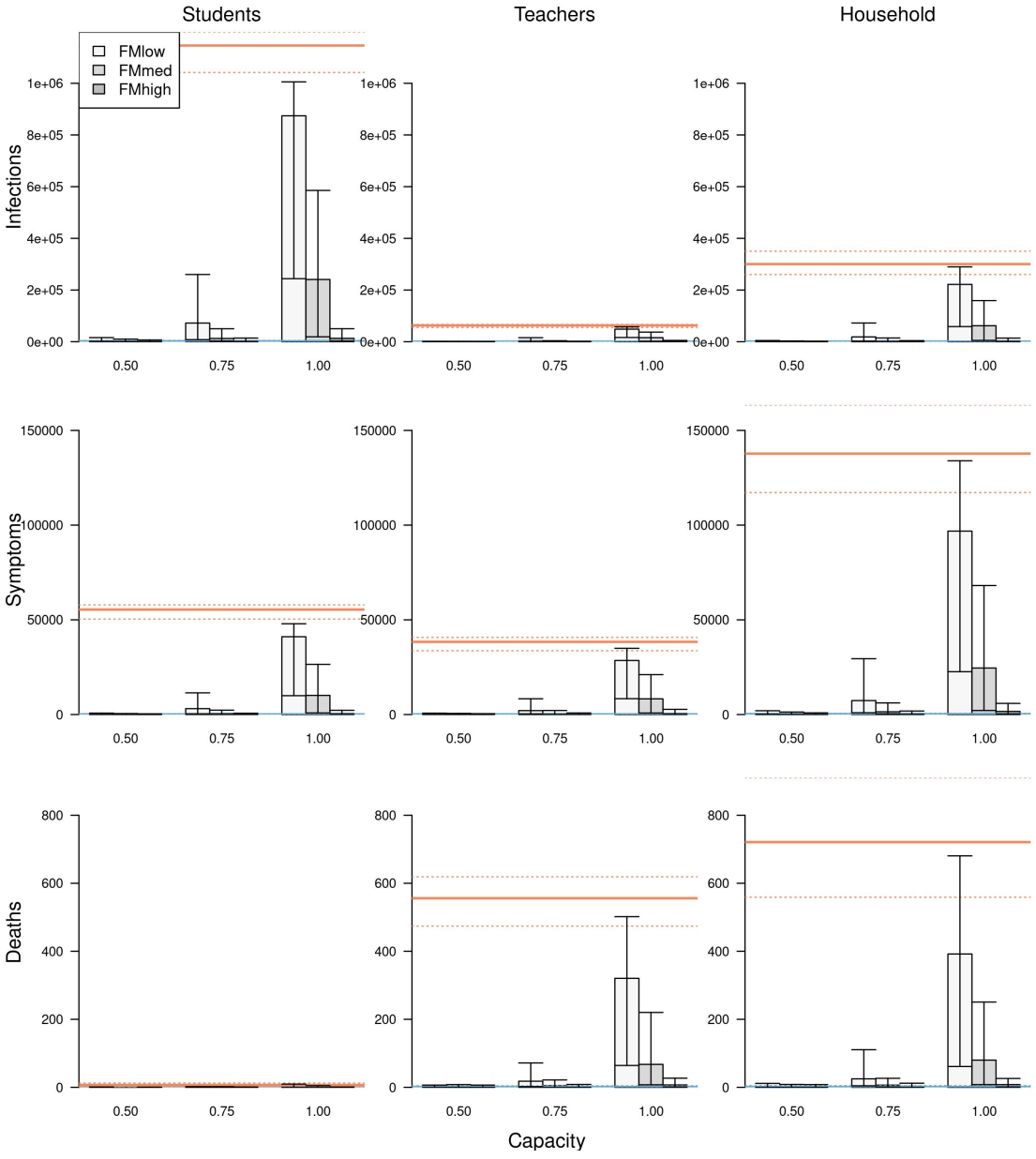

Figure 5. The impact of different school reopening strategies on cumulative infections (top row), cumulative symptomatic infections (middle row), and cumulative deaths (bottom row) in Indiana between August 24 and December 31. These outcomes are presented separately for students (left column), teachers (middle column), and school-affiliated families (right column). Scenarios are defined by the capacity at which schools operate (x-axis) and face-mask adherence (shading). Orange lines represent projections under a scenario of school reopening at full capacity without masks (solid: median; dotted: 95% posterior predictive interval). Blue lines represent a scenario where schools operate remotely. Error bars indicate inter-quartile ranges.

References

[1] The New York Times. "Coronavirus in the U.S.: Latest Map and Case Count". en-US. In: *The New York Times* (July 2020). ISSN: 0362-4331.

[2] H Juliette T Unwin et al. "State-Level Tracking of COVID-19 in the United States". In: *medRxiv* (2020). DOI: 10.1101/2020.07.13.20152355. eprint: https://www.medrxiv.org/content/early/2020/07/14/2020.07.13.20152355.full.pdf.

[3] Seth Flaxman et al. "Estimating the Effects of Non-Pharmaceutical Interventions on COVID-19 in Europe". In: *Nature* 584.7820 (Aug. 2020), pp. 257–261. ISSN: 1476-4687. DOI: 10.1038/s41586-020-2405-7.

[4] *Coronavirus Government Response Tracker*. en. https://www.bsg.ox.ac.uk/research/research-projects/coronavirus-government-response-tracker.

[5] Hamada S Badr et al. "Association between Mobility Patterns and COVID-19 Transmission in the USA: A Mathematical Modelling Study". In: *The Lancet Infectious Diseases* (2020). ISSN: 1473-3099. DOI: 10.1016/S1473-3099(20)30553-3.

[6] Katherine A. Auger et al. "Association between Statewide School Closure and COVID-19 Incidence and Mortality in the US". In: *JAMA* (July 2020). ISSN: 0098-7484. DOI: 10.1001/jama.2020.14348.

[7] Charles Courtemanche et al. "Strong Social Distancing Measures In The United States Reduced The COVID-19 Growth Rate: Study Evaluates the Impact of Social Distancing Measures on the Growth Rate of Confirmed COVID-19 Cases across the United States." In: *Health Affairs* (2020), pp. 10–1377.

[8] *ISDH - Novel Coronavirus: Indiana COVID-19 Dashboard*. https://www.coronavirus.in.gov/2393.htm.

[9] Kenne A. Dibner, Heidi A. Schweingruber, and Dimitri A. Christakis. "Reopening K-12 Schools during the COVID-19 Pandemic: A Report from the National Academies of Sciences, Engineering, and Medicine". In: *JAMA* (July 2020). ISSN: 0098-7484. DOI: 10.1001/jama.2020.14745.

[10] *President Donald J. Trump Is Supporting America's Students and Families By Encouraging the Safe Reopening of America's Schools*. en-US. https://www.whitehouse.gov/briefings-statements/president-donald-j-trump-supporting-americas-students-families-encouraging-safe-reopening-americas-schools/.

[11] Indiana State Department of Health, Indiana Department of Education, and Indiana Family and Social Services Administration. *IN-CLASS: Indiana's Considerations for Learning and Safe Schools. COVID-19 Health and Safety Re-Entry Guidance.* June 2020.

[12] Charlotte Jackson et al. "School Closures and Influenza: Systematic Review of Epidemiological Studies". In: *BMJ Open* 3.2 (2013). ISSN: 2044-6055. DOI: 10.1136/bmjopen-2012-002149. eprint: https://bmjopen.bmj.com/content/3/2/e002149.full.pdf.

[13] Shoko Kawano and Masayuki Kakehashi. "Substantial Impact of School Closure on the Transmission Dynamics during the Pandemic Flu H1N1-2009 in Oita, Japan". In: *PLOS ONE* 10.12 (Dec. 2015), pp. 1–15. DOI: 10.1371/journal.pone.0144839.

[14] Simon Cauchemez et al. "Closure of Schools during an Influenza Pandemic". In: *The Lancet Infectious Diseases* 9.8 (2009), pp. 473–481. ISSN: 1473-3099. DOI: 10.1016/S1473-3099(09)70176-8.

[15] Niel Hens et al. "Estimating the Impact of School Closure on Social Mixing Behaviour and the Transmission of Close Contact Infections in Eight European Countries". In: *BMC infectious diseases* 9.1 (2009), p. 187.

[16] Simon Cauchemez et al. "Estimating the Impact of School Closure on Influenza Transmission from Sentinel Data". In: *Nature* 452.7188 (Apr. 2008), pp. 750–754. ISSN: 1476-4687. DOI: 10.1038/nature06732.

[17] Charlotte Jackson et al. "The Effects of School Closures on Influenza Outbreaks and Pandemics: Systematic Review of Simulation Studies". In: *PLOS ONE* 9.5 (May 2014), pp. 1–10. DOI: 10.1371/journal.pone.0097297.

[18] Sten H Vermund and Virginia E Pitzer. "Asymptomatic Transmission and the Infection Fatality Risk for COVID-19: Implications for School Reopening". In: *Clinical Infectious Diseases* (June 2020). ISSN: 1058-4838. DOI: 10.1093/cid/ciaa855.

[19] Nicholas G. Davies et al. "Age-Dependent Effects in the Transmission and Control of COVID-19 Epidemics". In: *Nature Medicine* (June 2020). ISSN: 1546-170X. DOI: 10.1038/s41591-020-0962-9.

[20] Juanjuan Zhang et al. "Changes in Contact Patterns Shape the Dynamics of the COVID-19 Outbreak in China". In: *Science* 368.6498 (2020), pp. 1481–1486. ISSN: 0036-8075. DOI: 10.1126/science.abb8001. eprint: https://science.sciencemag.org/content/368/6498/1481.full.pdf.

[21] Joseph T Wu et al. "Estimating Clinical Severity of COVID-19 from the Transmission Dynamics in Wuhan, China". In: *Nature medicine* (2020), pp. 1–5.

[22] Robert Verity et al. "Estimates of the Severity of Coronavirus Disease 2019: A Model-Based Analysis". eng. In: *The Lancet. Infectious Diseases* (Mar. 2020). ISSN: 1474-4457. DOI: 10.1016/S1473-3099(20)30243-7.

[23] Willem et al. "The Impact of Contact Tracing and Household Bubbles on Deconfinement Strategies for COVID-19: An Individual-Based Modelling Study". In: *medRxiv* (2020). DOI: 10.1101/2020.07.01.20144444. eprint: https://www.medrxiv.org/content/early/2020/07/06/2020.07.01.20144444.full.pdf.

[24] Christine M Szablewski. "SARS-CoV-2 Transmission and Infection among Attendees of an Overnight Camp—Georgia, June 2020". In: *MMWR. Morbidity and mortality weekly report* 69 (2020), pp. 1023–1025. DOI: http://dx.doi.org/10.15585/mmwr.mm6931e1.

[25] Young Joon Park et al. "Contact Tracing during Coronavirus Disease Outbreak, South Korea, 2020". In: *Emerging Infectious Disease journal* 26.10 (2020). ISSN: 1080-6059. DOI: 10.3201/eid2610.201315.

[26] Pirous Fateh-Moghadam et al. "Contact Tracing during Phase I of the COVID-19 Pandemic in the Province of Trento, Italy: Key Findings and Recommendations". In: *medRxiv* (2020). DOI: 10.1101/2020.07.16.20127357. eprint: https://www.medrxiv.org/content/early/2020/07/29/2020.07.16.20127357.full.pdf.

[27] George Psacharopoulos et al. "Lost Wages: The COVID-19 Cost of School Closures". In: *World Bank Policy Research Working Paper* 9246 (2020).

[28] Danielle G. Dooley, Asad Bandealy, and Megan M. Tschudy. "Low-Income Children and Coronavirus Disease 2019 (COVID-19) in the US". In: *JAMA Pediatrics* (May 2020). ISSN: 2168-6203. DOI: 10.1001/jamapediatrics.2020.2065. eprint: https://jamanetwork.com/journals/jamapediatrics/articlepdf/2766115/jamapediatrics\textbackslash_dooley\textbackslash_2020\textbackslash_vp\textbackslash_200021.pdf.

[29] Wim Van Lancker and Zachary Parolin. "COVID-19, School Closures, and Child Poverty: A Social Crisis in the Making". In: *The Lancet Public Health* 5.5 (2020), e243–e244.

[30] John J Grefenstette et al. "FRED (A Framework for Reconstructing Epidemic Dynamics): An Open-Source Software System for Modeling Infectious Diseases and Control Strategies Using Census-Based Populations". In: *BMC public health* 13.1 (2013), p. 940.

[31] Derek K Chu et al. "Physical Distancing, Face Masks, and Eye Protection to Prevent Person-to-Person Transmission of SARS-CoV-2 and COVID-19: A Systematic Review and Meta-Analysis". In: *The Lancet* (2020).

[32] W D Wheaton. "2005-2009 U.S. Synthetic Population Ver.2. RTI International". In: (2012).

[33] Joël Mossong et al. "Social Contacts and Mixing Patterns Relevant to the Spread of Infectious Diseases". In: *PLOS Medicine* 5.3 (Mar. 2008), pp. 1–1. DOI: 10.1371/journal.pmed.0050074.

[34] Tapiwa Ganyani et al. "Estimating the Generation Interval for COVID-19 Based on Symptom Onset Data". en. In: *medRxiv* (Mar. 2020), p. 2020.03.05.20031815. ISSN: 10.1101/2020.03.05.20031815. DOI: 10.1101/2020.03.05.20031815.

[35] Kenji Mizumoto et al. "Estimating the Asymptomatic Proportion of Coronavirus Disease 2019 (COVID-19) Cases on Board the Diamond Princess Cruise Ship, Yokohama, Japan, 2020". en. In: *Eurosurveillance* 25.10 (Mar. 2020), p. 2000180. ISSN: 1560-7917. DOI: 10.2807/1560-7917.ES.2020.25.10.2000180.

[36] Lael M. Yonker et al. "Pediatric SARS-CoV-2: Clinical Presentation, Infectivity, and Immune Responses". In: *The Journal of Pediatrics* (). ISSN: 0022-3476. DOI: 10.1016/j.jpeds.2020.08.037.

[37] Taylor Heald-Sargent et al. "Age-Related Differences in Nasopharyngeal Severe Acute Respiratory Syndrome Coronavirus 2 (SARS-CoV-2) Levels in Patients with Mild to Moderate Coronavirus Disease 2019 (COVID-19)". In: *JAMA Pediatrics* (July 2020). ISSN: 2168-6203. DOI: 10.1001/jamapediatrics.2020.3651. eprint: https://jamanetwork.com/journals/jamapediatrics/articlepdf/2768952/jamapediatrics\textbackslash_healdsargent\textbackslash_2020\textbackslash_ld\textbackslash_200036.pdf.

[38] Shixiong Hu et al. "Infectivity, Susceptibility, and Risk Factors Associated with SARS-CoV-2 Transmission under Intensive Contact Tracing in Hunan, China". In: *medRxiv* (2020). DOI: 10.1101/2020.07.23.20160317. eprint: https://www.medrxiv.org/content/early/2020/08/07/2020.07.23.20160317.full.pdf.

[39] Stephen A. Lauer et al. "The Incubation Period of Coronavirus Disease 2019 (COVID-19) From Publicly Reported Confirmed Cases: Estimation and Application". en. In: *Annals of Internal Medicine* (Mar. 2020). ISSN: 0003-4819. DOI: 10.7326/M20-0504.

[40] Qifang Bi et al. "Epidemiology and Transmission of COVID-19 in 391 Cases and 1286 of Their Close Contacts in Shenzhen, China: A Retrospective Cohort Study". In: *The Lancet Infectious Diseases* (2020).

[41] The Novel Coronavirus Pneumonia Emergency Response Epidemiology Team. "The Epidemiological Characteristics of an Outbreak of 2019 Novel Coronavirus Diseases (COVID-19) — China, 2020". en. In: *China CDC Weekly* 2.8 (Feb. 2020), pp. 113–122. ISSN: 2096-7071.

[42] T Alex Perkins et al. "Calling in Sick: Impacts of Fever on Intra-Urban Human Mobility". In: *Proceedings of the Royal Society of London B: Biological Sciences* 283.1834 (2016). ISSN: 0962-8452. DOI: 10.1098/rspb.2016.0390.

[43] Team CDC COVID et al. "Characteristics of Health Care Personnel with COVID-19-United States, February 12-April 9, 2020." In: *MMWR. Morbidity and Mortality Weekly Report* (2020).

[44] IHME COVID-19 health service utilization forecasting Team and Christopher JL Murray. "Forecasting COVID-19 Impact on Hospital Bed-Days, ICU-Days, Ventilator-Days and Deaths by US State in the next 4 Months". en. In: *medRxiv* (Mar. 2020), p. 2020.03.27.20043752. DOI: 10.1101/2020.03.27.20043752.

[45] *COVID-19 Community Mobility Report*. https://www.google.com/covid19/mobility?hl=en.

[46] Christopher J Cronin and William N Evans. *Private Precaution and Public Restrictions: What Drives Social Distancing and Industry Foot Traffic in the COVID-19 Era?* Working Paper 27531. National Bureau of Economic Research, July 2020. DOI: 10.3386/w27531.

[47] *Google Trends*. en-US. https://trends.google.com/trends/?geo=US.

[48] New York Times and Dynata. *Estimates from The New York Times, Based on Roughly 250,000 Interviews Conducted by Dynata from July 2 to July 14*. Tech. rep.

[49] The COVID Tracking Project. *Michigan*. en. https://covidtracking.com/data/state/michigan. 2020.

[50] Aaron A. King et al. *pomp: Statistical Inference for Partially Observed Markov Processes*. Manual. 2020.

[51] Aaron A. King, Dao Nguyen, and Edward L. Ionides. "Statistical Inference for Partially Observed Markov Processes via the R Package pomp". In: *Journal of Statistical Software* 69.12 (2016), pp. 1–43. DOI: 10.18637/jss.v069.i12.

[52] Nir Menachemi et al. "Population Point Prevalence of SARS-CoV-2 Infection Based on a Statewide Random Sample—Indiana, April 25–29, 2020". In: *Morbidity and Mortality Weekly Report* 69.29 (2020), p. 960.

[53] Andrea Zeek. *COVID-19 Study's Phase 2 Results Show Spread of Virus in Indiana*. en. https://news.iu.edu/stories/2020/06/iupui/releases/17-fairbanks-isdh-second-phase-covid-19-testing-indiana-research.html. June 2020.

[54] T. Alex Perkins et al. "Estimating Unobserved SARS-CoV-2 Infections in the United States". In: *Proceedings of the National Academy of Sciences* (2020). ISSN: 0027-8424. DOI: 10.1073/pnas.2005476117. eprint: https://www.pnas.org/content/early/2020/08/20/2005476117.full.pdf.

[55] *MIDAS Network, Midas-Network/COVID-19*. GitHub. https://github.com/midas-net-work/COVID-19.

[56] Susanna Esposito and Nicola Principi. "School Closure during the Coronavirus Disease 2019 (COVID-19) Pandemic: An Effective Intervention at the Global Level?" In: *JAMA Pediatrics* (May 2020). ISSN: 2168-6203. DOI: 10.1001/jamapediatrics.2020.1892. eprint: https://jamanetwork.com/journals/jamapediatrics/articlepdf/2766114/jamapediatrics\textbackslash_esposito\textbackslash_2020\textbackslash_vp\textbackslash_200019.pdf.

[57] Nor Fazila Che Mat et al. "A Single Mass Gathering Resulted in Massive Transmission of COVID-19 Infections in Malaysia with Further International Spread". In: *Journal of Travel Medicine* 27.3 (Apr. 2020). ISSN: 1708-8305. DOI: 10.1093/jtm/taaa059. eprint: https://academic.oup.com/jtm/article-pdf/27/3/taaa059/33226391/taaa059.pdf.

[58] Sukbin Jang, Si Hyun Han, and Ji-Young Rhee. "Cluster of Coronavirus Disease Associated with Fitness Dance Classes, South Korea". eng. In: *Emerging infectious diseases* 26.8 (Aug. 2020), pp. 1917–1920. ISSN: 1080-6059. DOI: 10.3201/eid2608.200633.

[59] Matt J Keeling et al. "The Impact of School Reopening on the Spread of COVID-19 in England". In: *medRxiv* (2020). DOI: 10.1101/2020.06.04.20121434. eprint: https://www.medrxiv.org/content/early/2020/06/05/2020.06.04.20121434.full.pdf.

[60] Jennifer R Head et al. "The Effect of School Closures and Reopening Strategies on COVID-19 Infection Dynamics in the San Francisco Bay Area: A Cross-Sectional Survey and Modeling Analysis". In: *medRxiv* (2020). DOI: 10.1101/2020.08.06.20169797. eprint: https://www.medrxiv.org/content/early/2020/08/07/2020.08.06.20169797.full.pdf.

[61] Jasmina Panovska-Griffiths et al. "Determining the Optimal Strategy for Reopening Schools, the Impact of Test and Trace Interventions, and the Risk of Occurrence of a Second COVID-19 Epidemic Wave in the UK: A Modelling Study". In: *The Lancet Child & Adolescent Health* (2020). ISSN: 2352-4642. DOI: 10.1016/S2352-4642(20)30250-9.

[62] Benjamin Lee et al. "Modeling the Impact of School Reopening on SARS-CoV-2 Transmission". In: *Research Square* (2020).

[63] Alfonso Landeros et al. "An Examination of School Reopening Strategies during the SARS-CoV-2 Pandemic". In: *medRxiv* (2020). DOI: 10.1101/2020.08.05.20169086. eprint: https://www.medrxiv.org/content/early/2020/08/06/2020.08.05.20169086.full.pdf.

[64] Richard OJH Stutt et al. "A Modelling Framework to Assess the Likely Effectiveness of Facemasks in Combination with 'Lock-down'in Managing the COVID-19 Pandemic". In: *Proceedings of the Royal Society A* 476.2238 (2020), p. 20200376.

[65] *COVID-19 Hospitalizations*. https://gis.cdc.gov/grasp/COVIDNet/COVID19_3.html.

[66] Enrico Lavezzo et al. "Suppression of a SARS-CoV-2 Outbreak in the Italian Municipality of Vo'". In: *Nature* 584.7821 (Aug. 2020), pp. 425–429. ISSN: 1476-4687. DOI: 10.1038/s41586-020-2488-1.

[67] Terry C Jones et al. "An Analysis of SARS-CoV-2 Viral Load by Patient Age". In: *medRxiv* (2020). DOI: 10.1101/2020.06.08.20125484. eprint: https://www.medrxiv.org/content/early/2020/06/09/2020.06.08.20125484.full.pdf.

[68] Itai Dattner et al. "The Role of Children in the Spread of COVID-19: Using Household Data from Bnei Brak, Israel, to Estimate the Relative Susceptibility and Infectivity of Children". In: *medRxiv* (2020). DOI: 10.1101/2020.06.03.20121145. eprint: https://www.medrxiv.org/content/early/2020/06/05/2020.06.03.20121145.full.pdf.

[69] Chen Stein-Zamir et al. "A Large COVID-19 Outbreak in a High School 10 Days after Schools' Reopening, Israel, May 2020". In: *Eurosurveillance* 25.29 (2020), p. 2001352. DOI: 10.2807/1560-7917.ES.2020.25.29.2001352.

[70] Hannah Reed. "Some school districts in Northwest Indiana are reporting COVID-19 cases and quarantined students". English (United States), en-US. In: *Chicago Tribune* ().

[71] Elaheh Abdollahi et al. "Simulating the Effect of School Closure during COVID-19 Outbreaks in Ontario, Canada". In: *BMC Medicine* 18.1 (July 2020), p. 230. ISSN: 1741-7015. DOI: 10.1186/s12916-020-01705-8.

Supplementary material

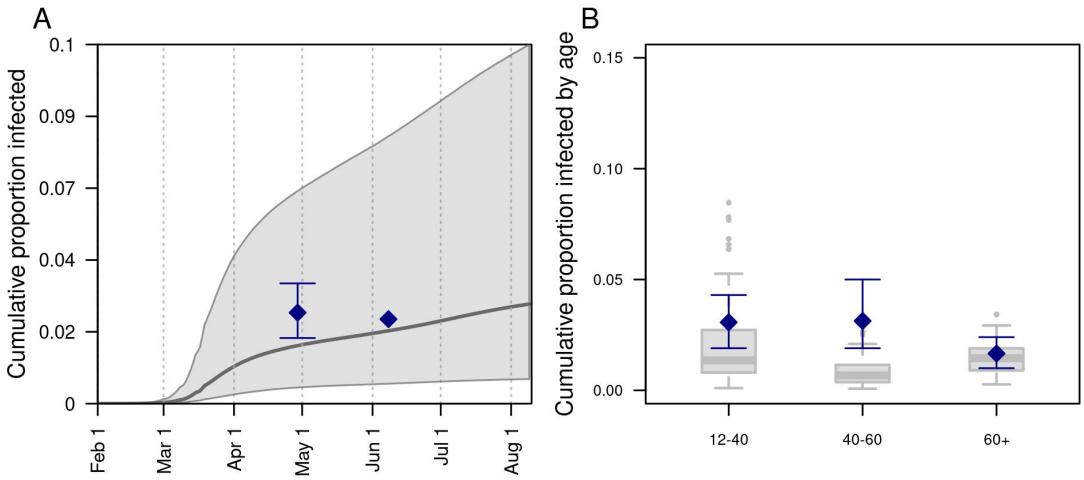

Figure S1. Model comparison with data withheld from fitting. We validated the model's predictions against data withheld from fitting on A) the cumulative proportion of the population of Indiana infected through late April and early June, and B) the cumulative proportion infected among individuals aged 12-40, 40-60, and 60+. Data are shown in navy and come from a random, statewide serological survey [52]. Model predictions are shown in gray. In A, the line and band indicate the median and 95% posterior predictive interval. In B, lines, boxes, and error bars indicate median, interquartile range, and 95% posterior predictive interval.

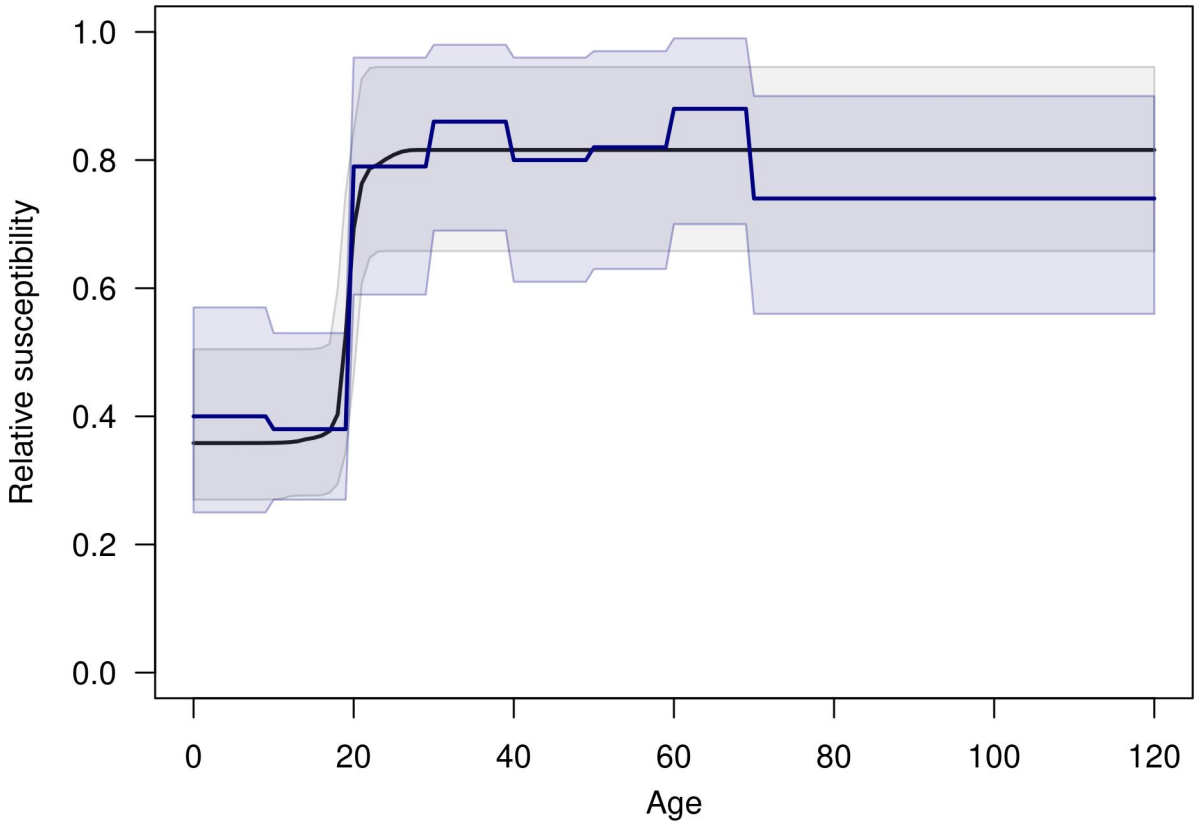

Figure S2. Susceptibility to SARS-CoV-2 infection by age. The black line shows the median of the estimated curve of susceptibility by age, which took the form of a modified logistic function defined by four parameters: minimum, maximum, inflection point, and slope. The gray band represents the 95% credible interval. Navy lines show estimates from Davies et al. [19] that were used to inform our estimates.

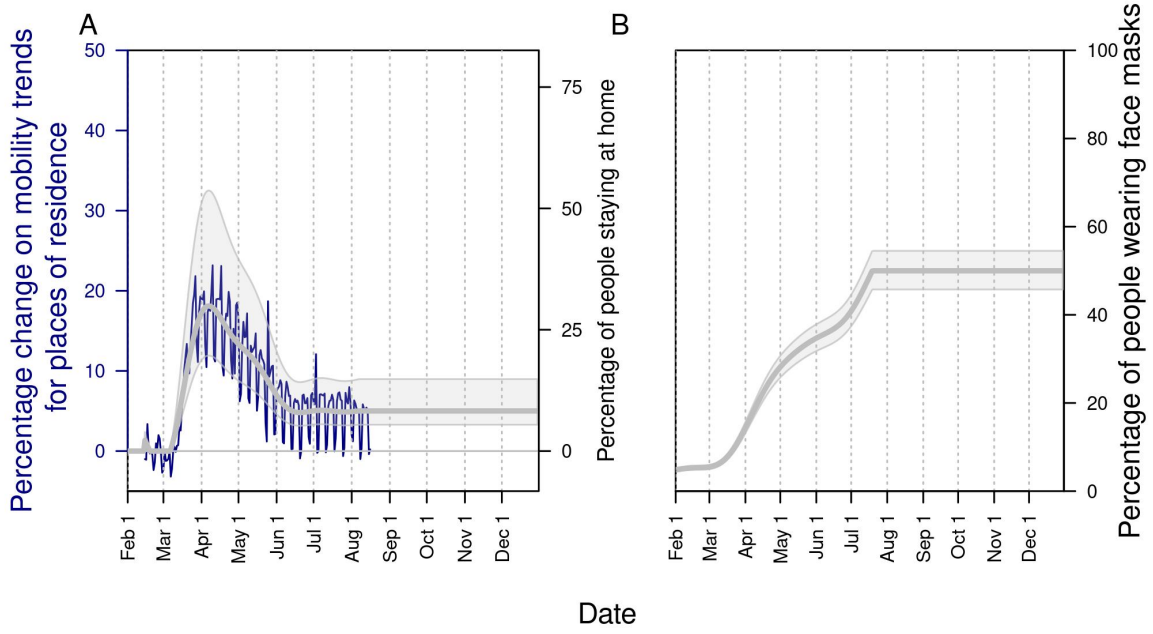

Figure S3. Changes in A) mobility patterns over time and B) face-mask adherence in the community as a whole. In A, the gray line shows the fitted pattern for the Google mobility index related to residential locations (navy line). Adherence to shelter-in-place in the model follows the same trend, but with its magnitude estimated through the model calibration process. In B, the gray line is informed by fitting to Google search data on "face mask" and assuming that values plateau from July 19 onward at a value informed by survey data [47, 48]

.

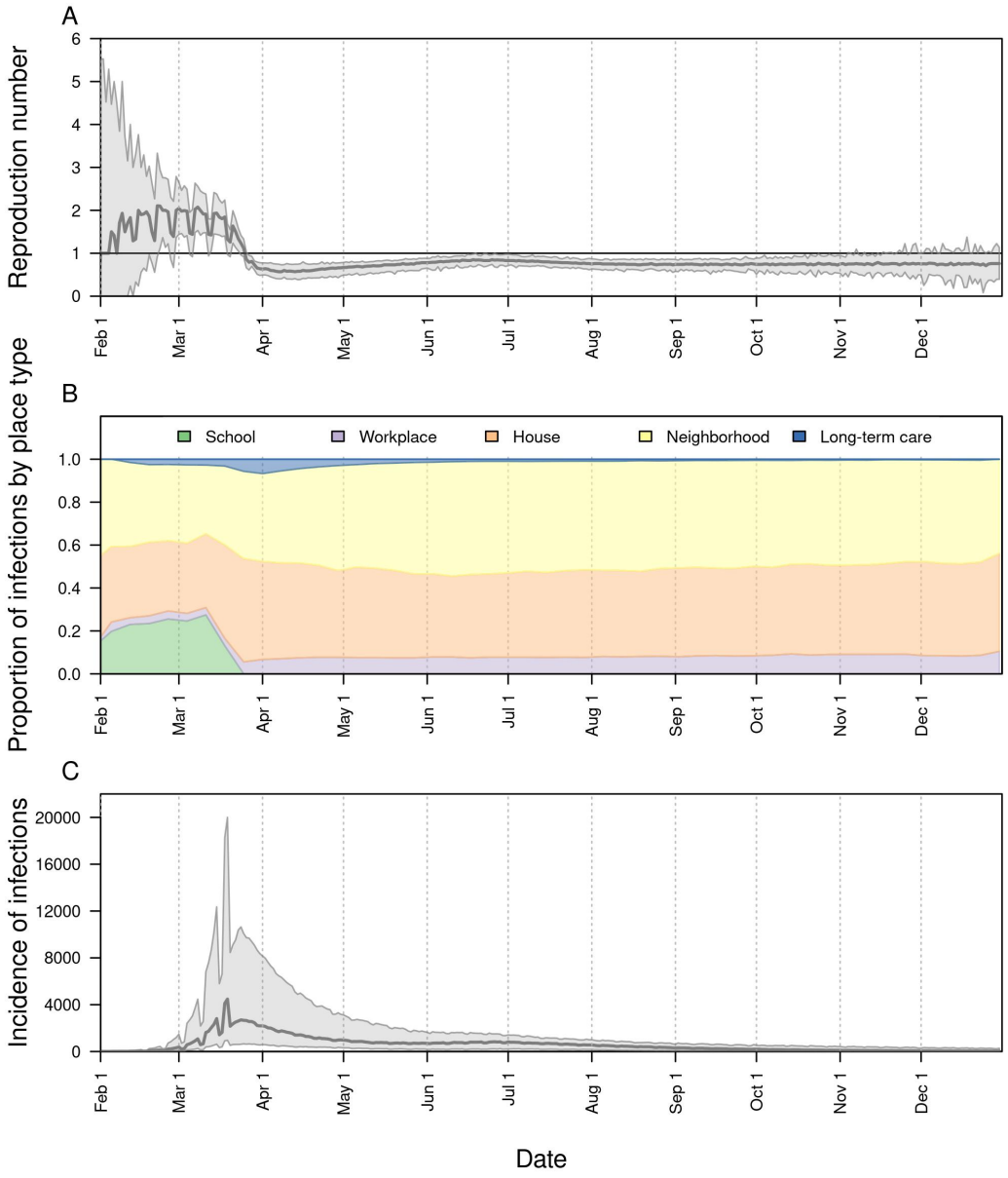

Figure S4. The impact of remote instruction in schools in Indiana on: A) the reproduction number, $R(t)$, over time; B) the proportion of infections acquired in different location types over time; and C) the daily incidence of infection over time. In A and C, the line represents the median, and the shaded region represents the 50% posterior predictive interval.

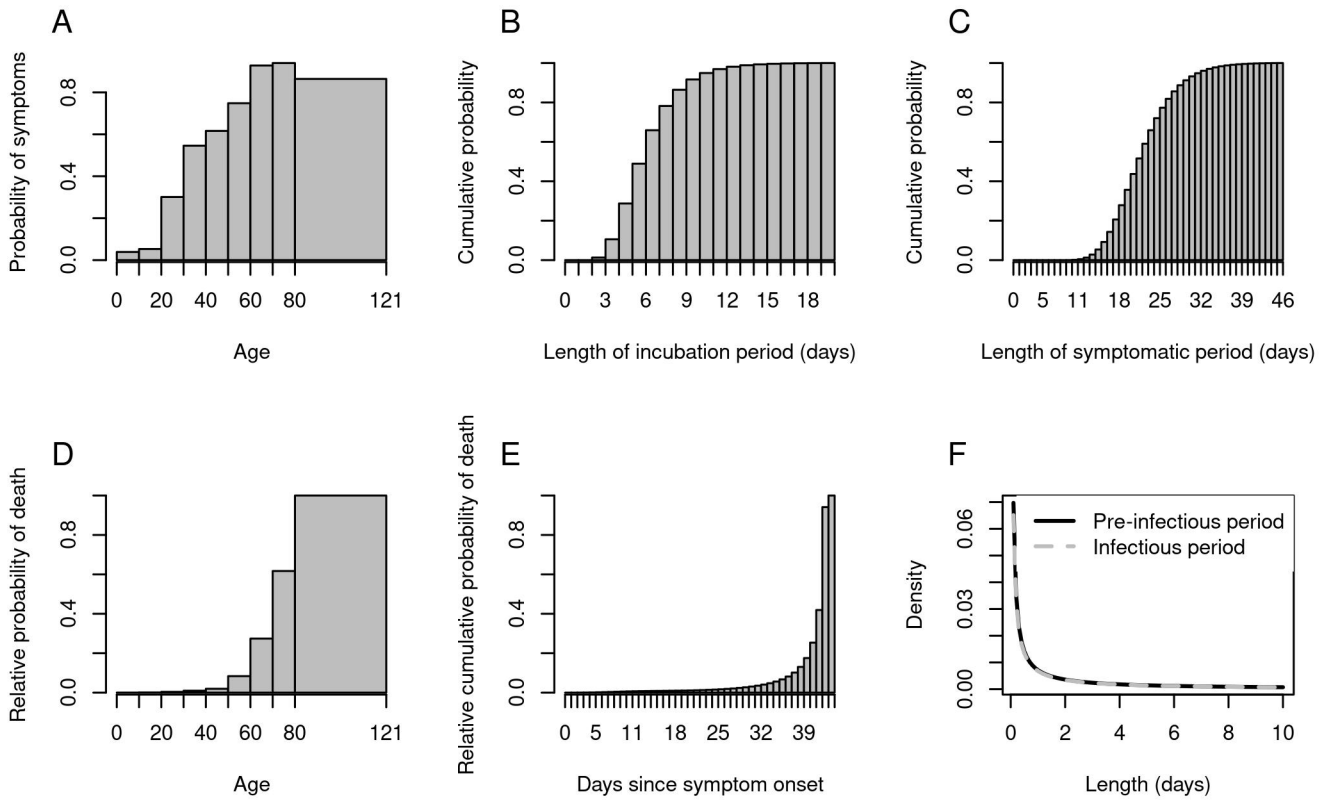

Figure S5. Distributions for parameters in the model. The probability of death is a product of the age-stratified relative probability of death and the daily relative probability of death, conditional on the individual still having symptoms by that day.

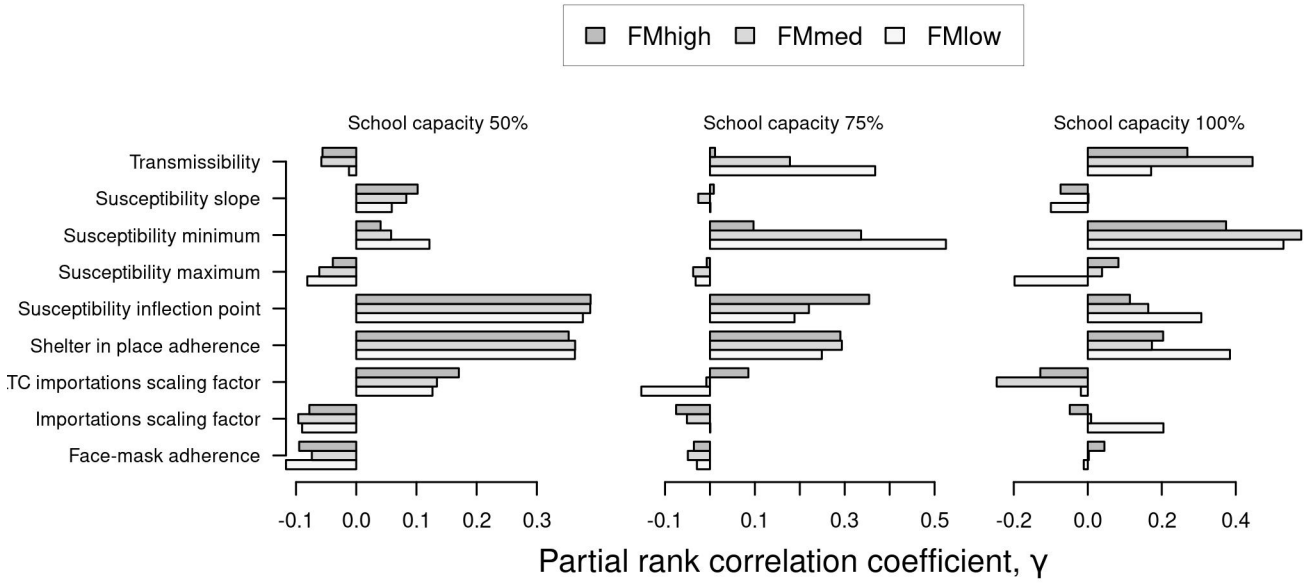

Figure S6. Sensitivity analysis of cumulative infections statewide between August 24 and December 31 to variation in the model's nine parameters. Bars indicate values of the partial rank correlation coefficient. Results are presented separately by school operating capacity (panels) and face-mask adherence in schools (gray shading).

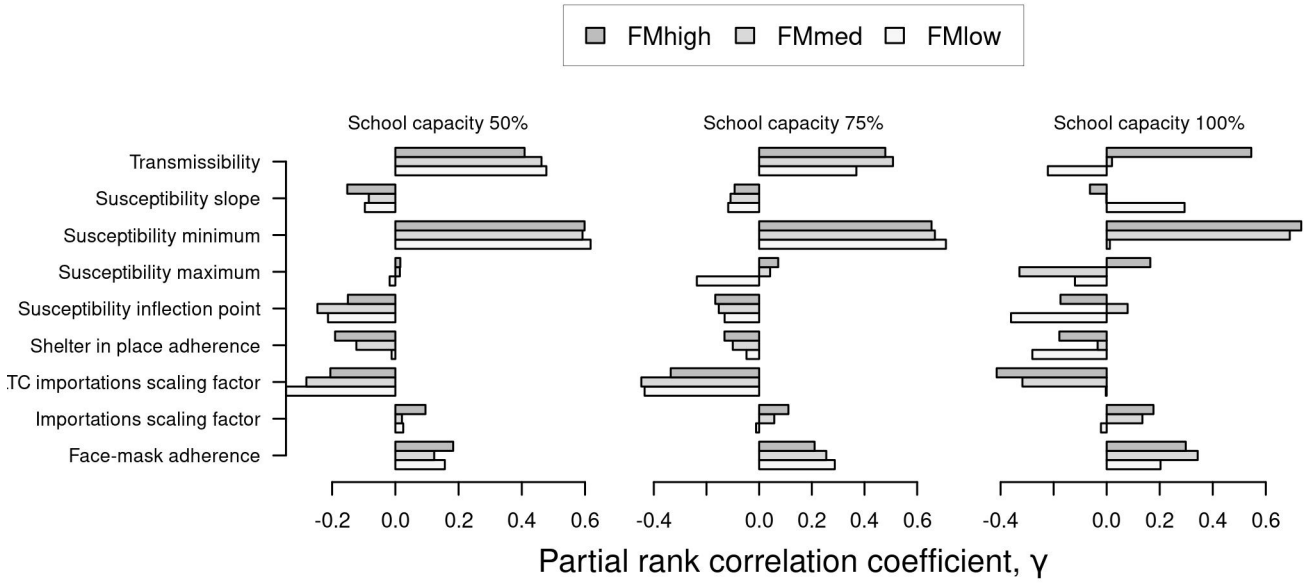

Figure S7. Sensitivity analysis of the proportion of infections acquired in schools between August 24 and December 31 to variation in the model's nine parameters. Bars indicate values of the partial rank correlation coefficient. Results are presented separately by school operating capacity (panels) and face-mask adherence in schools (gray shading).

Capacity	Facemask	Cumulative infections	Cumulative deaths
0.50	Low	1.5 (1.4-1.6)	1.2 (1.1-1.2)
0.50	Med	1.3 (1.2-1.3)	1.1 (1.0-1.1)
0.50	High	1.1 (1.1-1.2)	1.0 (1.0-1.1)
0.75	Low	10.9 (10.2-11.5)	2.6 (2.5-2.8)
0.75	Med	2.8 (2.7-3.0)	1.5 (1.4-1.6)
0.75	High	1.4 (1.3-1.5)	1.2 (1.1-1.2)
1.00	Low	81.8 (78.3-85.3)	13.4 (12.8-14.0)
1.00	Med	29.5 (27.9-31.1)	5.0 (4.8-5.2)
1.00	High	3.0 (2.8-3.1)	1.5 (1.5-1.6)

Table S1. Proportional increase in risk for the overall population of Indiana under alternative scenarios about school operating capacity and face-mask adherence in schools. We define the proportional increase in risk as the ratio of the cumulative number of events (infections or deaths) between August 24 and December 31 under the scenario indicated by the left two columns as compared to a scenario in which schools operate remotely.

Capacity	Facemask	Student infections	Student symptoms
0.50	Low	3.0 (2.8-3.1)	2.7 (2.5-2.8)
0.50	Med	2.0 (1.9-2.1)	1.8 (1.7-1.9)
0.50	High	1.4 (1.3-1.5)	1.3 (1.3-1.4)
0.75	Low	55.3 (52.1-58.7)	43.4 (40.7-46.0)
0.75	Med	9.2 (8.7-9.7)	7.8 (7.3-8.3)
0.75	High	2.6 (2.4-2.7)	2.3 (2.2-2.5)
1.00	Low	471.2 (450.8-491.6)	405.3 (387.6-420.8)
1.00	Med	165.4 (156.3-175.0)	131.8 (124.9-139.0)
1.00	High	9.7 (9.1-10.3)	8.2 (7.7-8.7)

Table S2. Proportional increase in risk for students under alternative scenarios about school operating capacity and face-mask adherence in schools. We define the proportional increase in risk as the ratio of the cumulative number of events (infections or symptomatic infections) between August 24 and December 31 under the scenario indicated by the left two columns as compared to a scenario in which schools operate remotely.

Capacity	Facemask	Teacher infections	Teacher symptoms	Teacher deaths
0.50	Low	2.0 (1.8-2.1)	1.9 (1.8-2.0)	1.7 (1.6-1.9)
0.50	Med	1.5 (1.4-1.6)	1.5 (1.4-1.6)	1.5 (1.4-1.6)
0.50	High	1.3 (1.2-1.4)	1.3 (1.2-1.4)	1.3 (1.2-1.4)
0.75	Low	24.8 (23.3-26.5)	22.1 (20.6-23.6)	15.8 (14.6-17.1)
0.75	Med	5.3 (4.9-5.7)	5.0 (4.6-5.4)	4.7 (4.3-5.1)
0.75	High	2.1 (1.9-2.2)	2.1 (1.9-2.2)	1.8 (1.6-1.9)
1.00	Low	229.4 (218.1-239.9)	229.0 (218.4-239.9)	227.7 (213.3-244.0)
1.00	Med	83.5 (78.8-88.7)	76.8 (72.5-81.3)	58.4 (54.0-62.9)
1.00	High	6.8 (6.3-7.3)	6.5 (6.1-7.0)	6.1 (5.7-6.7)

Table S3. Proportional increase in risk for teachers under alternative scenarios about school operating capacity and face-mask adherence in schools. We define the proportional increase in risk as the ratio of the cumulative number of events (infections, symptomatic infections, or deaths) between August 24 and December 31 under the scenario indicated by the left two columns as compared to a scenario in which schools operate remotely.

Capacity	Facemask	Family infections	Family symptoms	Family deaths
0.50	Low	3.1 (2.9-3.3)	2.9 (2.8-3.1)	2.2 (2.0-2.4)
0.50	Med	2.1 (1.9-2.2)	2.0 (1.9-2.1)	1.6 (1.5-1.7)
0.50	High	1.5 (1.4-1.5)	1.4 (1.4-1.5)	1.4 (1.3-1.5)
0.75	Low	52.9 (49.7-56.5)	44.1 (41.5-46.9)	20.8 (19.4-22.5)
0.75	Med	9.4 (8.9-10.1)	8.4 (8.0-9.0)	5.6 (5.2-6.1)
0.75	High	2.7 (2.5-2.9)	2.6 (2.5-2.8)	2.2 (2.1-2.4)
1.00	Low	459.8 (439.3-480.6)	430.3 (413.1-448.9)	266.4 (251.9-283.3)
1.00	Med	157.1 (148.4-166.2)	133.8 (126.8-141.3)	63.8 (59.2-68.5)
1.00	High	10.0 (9.4-10.7)	9.0 (8.5-9.6)	6.1 (5.7-6.6)

Table S4. Proportional increase in risk for family members of students and teachers under alternative scenarios about school operating capacity and face-mask adherence in schools. We define the proportional increase in risk as the ratio of the cumulative number of events (infections, symptomatic infections, or deaths) between August 24 and December 31 under the scenario indicated by the left two columns as compared to a scenario in which schools operate remotely.

Capacity	Facemask	Cumulative infections	Cumulative deaths
0.50	Low	0.01 (0.01-0.01)	0.05 (0.05-0.05)
0.50	Med	0.01 (0.01-0.01)	0.05 (0.04-0.05)
0.50	High	0.01 (0.01-0.01)	0.04 (0.04-0.05)
0.75	Low	0.10 (0.09-0.10)	0.11 (0.11-0.11)
0.75	Med	0.02 (0.02-0.03)	0.06 (0.06-0.06)
0.75	High	0.01 (0.01-0.01)	0.05 (0.05-0.05)
1.00	Low	0.72 (0.71-0.73)	0.56 (0.54-0.57)
1.00	Med	0.26 (0.25-0.27)	0.21 (0.20-0.21)
1.00	High	0.03 (0.03-0.03)	0.06 (0.06-0.07)

Table S5. Overall proportional reduction in risk for the overall population of Indiana under alternative scenarios about school operating capacity and face-mask adherence in schools. We define the proportional reduction in risk as the ratio of the cumulative number of events (infections or deaths) between August 24 and December 31 under the scenario indicated by the left two columns as compared to a scenario in which schools operate at full capacity and without face masks.

Capacity	Facemask	Student infections	Student symptoms
0.50	Low	0.005 (0.004-0.005)	0.005 (0.004-0.005)
0.50	Med	0.003 (0.003-0.003)	0.003 (0.003-0.003)
0.50	High	0.002 (0.002-0.002)	0.002 (0.002-0.002)
0.75	Low	0.085 (0.081-0.089)	0.075 (0.072-0.078)
0.75	Med	0.014 (0.013-0.015)	0.013 (0.013-0.014)
0.75	High	0.004 (0.004-0.004)	0.004 (0.004-0.004)
1.00	Low	0.720 (0.709-0.730)	0.699 (0.687-0.709)
1.00	Med	0.253 (0.243-0.263)	0.228 (0.219-0.237)
1.00	High	0.015 (0.014-0.015)	0.014 (0.013-0.015)

Table S6. Proportional reduction in risk for students under alternative scenarios about school operating capacity and face-mask adherence in schools. We define the proportional reduction in risk as the ratio of the cumulative number of events (infections or symptomatic infections) between August 24 and December 31 under the scenario indicated by the left two columns as compared to a scenario in which schools operate at full capacity and without face masks.

Capacity	Facemask	Teacher infections	Teacher symptoms	Teacher deaths
0.50	Low	0.006 (0.006-0.007)	0.006 (0.005-0.006)	0.004 (0.004-0.004)
0.50	Med	0.005 (0.005-0.005)	0.005 (0.004-0.005)	0.004 (0.003-0.004)
0.50	High	0.004 (0.004-0.004)	0.004 (0.004-0.004)	0.003 (0.003-0.003)
0.75	Low	0.079 (0.075-0.082)	0.067 (0.064-0.070)	0.038 (0.037-0.040)
0.75	Med	0.017 (0.016-0.018)	0.015 (0.014-0.016)	0.011 (0.011-0.012)
0.75	High	0.007 (0.006-0.007)	0.006 (0.006-0.007)	0.004 (0.004-0.005)
1.00	Low	0.727 (0.718-0.737)	0.698 (0.687-0.708)	0.552 (0.540-0.565)
1.00	Med	0.265 (0.255-0.275)	0.234 (0.225-0.243)	0.142 (0.136-0.148)
1.00	High	0.022 (0.020-0.023)	0.020 (0.019-0.021)	0.015 (0.014-0.016)

Table S7. Proportional reduction in risk for teachers under alternative scenarios about school operating capacity and face-mask adherence in schools. We define the proportional reduction in risk as the ratio of the cumulative number of events (infections, symptomatic infections, or deaths) between August 24 and December 31 under the scenario indicated by the left two columns as compared to a scenario in which schools operate at full capacity and without face masks.

Capacity	Facemask	Family infections	Family symptoms	Family deaths
0.50	Low	0.005 (0.005-0.005)	0.005 (0.004-0.005)	0.004 (0.004-0.005)
0.50	Med	0.003 (0.003-0.003)	0.003 (0.003-0.003)	0.003 (0.003-0.003)
0.50	High	0.002 (0.002-0.002)	0.002 (0.002-0.002)	0.003 (0.003-0.003)
0.75	Low	0.082 (0.078-0.086)	0.069 (0.066-0.072)	0.042 (0.039-0.044)
0.75	Med	0.014 (0.014-0.015)	0.013 (0.013-0.014)	0.011 (0.011-0.012)
0.75	High	0.004 (0.004-0.004)	0.004 (0.004-0.004)	0.004 (0.004-0.005)
1.00	Low	0.705 (0.693-0.716)	0.674 (0.661-0.685)	0.533 (0.520-0.547)
1.00	Med	0.241 (0.232-0.251)	0.209 (0.201-0.218)	0.127 (0.122-0.133)
1.00	High	0.015 (0.015-0.016)	0.014 (0.013-0.015)	0.012 (0.012-0.013)

Table S8. Proportional reduction in risk for family members of students and teachers under alternative scenarios about school operating capacity and face-mask adherence in schools. We define the proportional reduction in risk as the ratio of the cumulative number of events (infections or deaths) between August 24 and December 31 under the scenario indicated by the left two columns as compared to a scenario in which schools operate at full capacity and without face masks.

Parameter	Value
Importations scaling factor	1.118 (95% CrI: 0.654-1.456)
Susceptibility slope	2.502 (95% CrI: 0.733-3.369)
Susceptibility minimum	0.401 (95% CrI: 0.275-0.437)
Susceptibility inflection point	19.648 (95% CrI: 17.644-20.548)
Susceptibility maximum	0.821 (95% CrI: 0.647-0.946)
Shelter in place adherence	0.382 (95% CrI: 0.252-0.687)
Face-mask adherence	0.500 (95% CrI: 0.458-0.545)
LTC importations scaling factor	0.046 (95% CrI: 0.007-0.093)
Transmissibility	0.641 (95% CrI: 0.546-0.965)
Probability of symptoms Age	Fig. S5A
Incubation period	Fig. S5B
Symptomatic period	Fig. S5C
Probability of death Age	Fig. S5D
Probability of death after symptom onset	Fig. S5E
Pre-infectious period	meanlog = 23.7, sdlog = 50 (Fig. S5F)
Infectious period	meanlog = 33.8, sdlog = 43.1 (Fig. S5F)
Adjusted odds ratio for face-mask efficacy	0.15[31]

Table S9. List of model parameters. The first nine were estimated through the model calibration process, and the subsequent seven were assumed based on the literature, as described in the Methods. Values of the first nine parameters reflect marginal posterior estimates.

Supplementary methods

Model description

People and their contacts

FRED simulates pathogen spread in a population by recreating interactions among people on a daily basis. To realistically represent the population of Indiana, we drew on a synthetic population of the US that represents demographic and geographic characteristics from 2010 [32]. Each human is modeled as an agent that visits a set of places defined by their activity space. This activity space contains places such as houses, schools, workplaces, and neighborhood locations. Transmission can occur when an infected person visits the same location as a susceptible person on the same day, with numbers of contacts per person specific to each location type. For instance, school contacts depend not on the size of the school but on the age of the student. We adopted contact rates specific to each location type that were previously calibrated to attack rates for influenza in each location type [30, 33].

Importation to seed local transmission

To initialize the model, we simulated international and domestic importations similar to Perkins et al. [54]. First, we obtained data on internationally and domestically imported deaths in Indiana up to March 18 [55], which we used to extrapolate total international and domestic importations based on the case fatality risk [41], the proportion of infections that are asymptomatic [35], and the probability of detecting local and international symptomatic infections [54]. Second, we assigned times to internationally imported infections proportional to international incidence patterns, adjusted to account for the timing of a ban on travel from China. We assigned times to domestically imported infections proportional to total US incidence. Drawing from uncertainty distributions for each of the three aforementioned parameters, we repeated this process 1,000 times and averaged across replicates. We used that average curve to seed our model, scaling its magnitude with a parameter that we calibrated. Although importations from outside Indiana likely continued beyond those that we were able to account for explicitly, we assumed that transmission within Indiana was sufficient at that point to be the primary driver of incidence. In addition to importations in the overall population, we simulated importation into long-term care facilities, given the large number of deaths that took place there and the limited realism of our model in simulating visitors to those facilities. We introduced infections into these facilities at a constant rate that we calibrated.

Transmission and disease progression

Once infected, each individual had latent and infectious periods drawn from distributions calibrated so that the average generation interval distribution matched estimates from Singapore ($\mu = 5.20, \sigma = 1.72$) [34]. The absolute risk of transmission depended on the number and location of an infected individual's contacts and a parameter that controls SARS-CoV-2 transmissibility upon contact, which we calibrated. We assumed asymptomatic infections were as infectious as

symptomatic infections and had identical timing of infectiousness [36, 37, 26, 38]. Following exposure, we assumed that children were less susceptible to infection than adults, which we modeled with a modified logistic function calibrated to results of Davies et al. [19]. We defined four parameters of this function as the *minimum* susceptibility, the *maximum* susceptibility, the *inflection point* of susceptibility with respect to age, and the *slope* of the age-susceptibility relationship around the inflection point. For agents that developed symptoms, we took random draws from lognormal distributions for the incubation period [39] and duration of symptoms [40]. Both the probabilities of developing symptoms [19] and dying [21] were assumed to increase with age. For infections that resulted in death, we modeled the time to death with a gamma distribution [22] truncated at the 99th percentile. These and other parameters are summarized in Table S9 and Fig. S5.

Changes in agent behavior during the epidemic

Agent behavior in FRED has the potential to change over the course of an epidemic. Following the onset of symptoms, infected agents self-isolate at home according to a fixed daily rate, whereas others continue their daily activities [42]. This rate is chosen so that on average 68% of agents will self-isolate at some point during their symptoms, assuming that all individuals who develop a fever will isolate at some point during their symptoms [43]. Agents can also respond to public health interventions, including school closure, shelter in place, and a combination of mask-wearing and social distancing. School closures occur on specific dates [44], resulting in students limiting their activity space to household and neighborhood locations. Shelter-in-place interventions reduce some agents' activity spaces to their households only, whereas others continue with their daily routines. We used mobility reports from Google [45] to drive daily compliance with shelter-in-place, such that shelter-in-place compliance in our model accounts for both the effects of shelter-in-place orders and some people deciding to continue staying at home after those orders are lifted [46]. To account for voluntary mask-wearing and social distancing, we used Google Trends data for Indiana using the terms "face mask" and "social distancing" [47] and used estimates on face-mask adherence from a New York Times analysis of a survey from Dynata [48].

Model calibration

We selected nine parameters to estimate based on calibration of the model to four data types on COVID-19 in Indiana: daily incidence of death, age distribution of deaths, daily incidence of hospitalization, and daily test positivity. The initial ranges for the statewide and long-term care facility importations were adjusted to cover a wide range of values. Compliance with shelter-in-place was informed with changes in mobility patterns in the Google community reports [45]. We fitted a GAM to the trends from the percentage change on mobility trends for places of residence, and projected the compliance of shelter-in-place orders after the period for which we had data by assuming a linear trend thereafter. We normalized these mobility trends from 0% (baseline) to 100% (everyone at home) and adjusted its magnitude with a parameter representing the maximum compliance in the historical trends. The minimum, maximum, inflection point,

and slope of the logistic function with which we model the age-susceptibility relationship were calibrated to estimates by Davies et al. [19].

We simulated 6,000 combinations of these nine parameters, $\vec{\theta}$, using a sobol design sampling algorithm with the sobolDesign function in R [50, 51]. For each parameter set, we calculated the likelihood of the model given the observed data on daily incidence of death, cumulative deaths in long-term care facilities through July 13, the decadal age distribution of cumulative deaths through July 13, daily incidence of hospitalization, and test positivity.

We calculated the contribution to the likelihood for daily incidence of death and cumulative deaths in long-term care facilities using a negative binomial distribution as

$$\mathcal{L}(\vec{\theta}|D_{t,k}) = \text{Negative Binomial}(r, p),$$

where $D_{t,k}$ is the daily incidence of death on day t and location k (long-term care facilities or all other locations), and r and p are size and probability parameters, respectively. We informed r and p using the conjugate prior relationship between a beta prior and negative binomial likelihood, such that $r = r_{prior} + d_{t,m}$ and $p = 1/(1 + \frac{p_{prior}}{p_{prior}+1})$, where $d_{t,m}$ is the daily incidence of death predicted by the model on day t. For the decadal age distribution of cumulative deaths through July 13, we used a multinomial distribution, such that

$$\mathcal{L}(\vec{\theta}|D_a) = \text{Multinomial}(D_a, d_{a,m}/\sum_a d_a),$$

where D_a is the observed number of deaths in the age group a, and $d_{a,m}$ are the deaths by age group obtained by the model. To fit to data on testing, we first observe, using Bayes' rule, that

$$\begin{aligned} P(C|T) &= \frac{P(T|C)P(C)}{P(T|C)P(C) + P(T|\neg C)P(\neg C)} \\ &= \frac{P(C)}{P(C) + r(1 - P(C))}, \end{aligned}$$

where C refers to a symptomatic case, T refers to an administered PCR test for current infection, and $r = P(T|\neg C)/P(T|C)$. Next, we assume that non-symptomatic infections (either presymptomatic or asymptomatic) exhibit treatment-seeking behavior similar to uninfected individuals, or $P(T|I) = P(T|U) = P(T|\neg C)$, where I refers to a non-symptomatic infection and U to uninfected. We then observe, again using Bayes' rule, that

$$P(I|T) = \frac{rP(I)}{P(C) + r(1 - P(C))}$$

and

$$P(U|T) = \frac{rP(U)}{P(C) + r(1 - P(C))}.$$

Next, we incorporate PCR sensitivity and specificity by assuming that sensitivity = $(P|C) = P(P|I)$, where P refers to a positive test (i.e., we assume that PCR sensitivity is similar for non-symptomatic and symptomatic infections). This allows us to write

$$P(P|T) = \text{sensitivity}(P(C|T) + P(I|T)) + (1 - \text{specificity})P(U|T).$$

Then, we are in a position to write the contribution to the likelihood from the testing data, assuming that the number of positive tests in the data, T_+, follows a binomial distribution

$$\mathcal{L}(\vec{\theta}|T_+, T_-) = \text{Binomial}(T_+ + T_-, P(P|T)),$$

where T_- represents the number of negative tests in the data.

Finally, the combined log-likelihood was obtained as

$$\log(\mathcal{L}(\vec{\theta})) = \sum_t \left(\log(\mathcal{L}(\vec{\theta}|D_{t,overall}))\right) + \log(\mathcal{L}(\vec{\theta}|D_{longtermcare}) + \log(\mathcal{L}(\vec{\theta}|T_+, T_-)) + \sum_a \left(\log(\mathcal{L}(\vec{\theta}|D_a)\right).$$

We sampled the parameters proportional to their likelihood to obtain a set of parameter combinations that constitute our approximation of the posterior distribution of parameter values.